SOA Gain Uniformity Improvement Employing a Non-Uniform Biasing Technique for Ultra-High Speed Optical Routers

A. Abd El Aziz[1], W. P. Ng[1], *Senior Member*, *IEEE*, Z. Ghassemlooy[1], *Senior Member*, *IEEE* ,
Moustafa H. Aly[2] and R. Ngah[3],
[1]*Optical Communications Research Group, NCRLab, Northumbria University, Newcastle upon Tyne, UK*
Tel: (+44)1912273841, e-mail: ahmed.shalaby@northumbria.ac.uk
[2]*Arab Academy for Science and Technology and Maritime Transport, Alexandria, Egypt*
[3]*Universiti Teknologi, Malaysia*

Abstract—In this paper, we propose a non-uniform biasing technique to improve the uniformity of the semiconductor optical amplifier (SOA) gain for ultra-high speed applications. In ultra-high speed applications, rapid gain recovery of the SOA is necessary to minimize the gain standard deviation and thus reducing system power penalties. A triangular shape biasing current is used in order to accelerate the SOA gain recovery while reducing the gain standard deviation. The effect of the non-uniform bias current on the SOA gain is investigated. The SOA is modeled using a segmentation method and the detailed theoretical analysis for the model is presented. The SOA gain and the output gain profiles achieved when injected with a burst of input Gaussian pulses for the non-uniform and the corresponding uniform techniques are also investigated. The operation principle is simulated and results show the boundaries and requirements in order to achieve the desired SOA bit rate for a range of different input powers. A reduction (at 1 mW input power) of 1.5 dB, 0.3 dB and 0.1 dB in the gain standard deviation is achieved for the input data rates of 10, 20 and 40 Gb/s, respectively.

Index Terms—carrier density, gain response, recovery time, semiconductor optical amplifier (SOA).

I. INTRODUCTION

Over the last decade, because of wavelength division multiplexing (WDM) and optical time division multiplexing (OTDM), the overall capacity of the point-to-point optical fiber transmission systems has been enormously increased by high-speed optoelectronic components. Accordingly, to overcome the speed and capacity bottleneck of optical-electrical-optical (OEO) conversion, there is a growing demand for ultrafast photonic networks that rely on photonic signal processing. The key processes in all-optical switching are regeneration and wavelength conversion where the SOA is the key element. Among all-optical switches, ultrafast all-optical switches based on SOA, such as Mach-Zehnder Interferometers (MZI) [1] are the most promising candidates for the realization of all-optical switching and processing applications because of their small size, low switching energy, high stability, fast and strong nonlinearity characteristics, and the potential of integration with other electronic and optical devices [2, 3].

SOA is also an important element for cascaded optical fiber systems and all-optical logic gates [4]. Nowadays, optical gates are used in almost all all-optical functions such as wavelength conversion, add-drop multiplexing (wavelength and time), clock recovery, regeneration, and simple bit-pattern recognition [5]. In addition, due to the lower cost and no requirement for optical isolators as often used in different types of amplifiers such as erbium doped fiber amplifiers (EDFAs) [4], SOAs are used as in-line amplifiers for bi-directional transmission in local and metropolitan systems and networks.

The performance of SOAs of any type is dictated, to a great extent, by their gain recovery time. To that end, for many high-speed applications, the SOA must have a fast gain recovery to avoid system penalties arising from bit pattern dependencies [6]. Fast gain recovery is also necessary at high-speed optical routers in order to achieve gain uniformity for high bit-rate input signals. The gain recovery of SOA is limited by the carrier lifetime, which itself depends on the applied or bias current [7]. Different approaches have been used to speed-up the recovery time by changing the cavity length of the SOA or by changing the input pulse width [8]. Several research groups have reported theoretical and experimental results on externally injected SOAs [6]. In [7] injection of an assist light at the transparency point of the SOA, which gives rise to very high speed operation at a current identical to that of a conventional SOA, was proposed.

Few work on non-uniform biasing have been reported in literatures using on and off impulses [9] and exponential shape current injections [10]. These were used to reduce the SOA switching time. However, the linearity of the output gain experienced by all input pulses has not been addressed. In [9] narrow current impulses were added with increasing amplitudes to the step signal. On the other hand, an exponential shape-current injection was used in order to reduce the turn-on time delay in an SOA switch in [10]. However the exponential biasing requires more energy applied to the SOA.

In this paper, we propose applying a triangular bias current to the SOA in order to improve the output gain uniformity compared to the uniform biasing scheme. We theoretically investigate the SOA total gain for both uniform and non-uniform biasing. The effect of the non-uniform bias current on the average gain, achieved by the input signal and the average gain deviation for different router speed, is simulated. The operation principle of the SOA is shown in the following section. Section III presents the mathematical analysis of the total gain and the change of the carrier density in terms of the rate and propagation equations. In section IV, the conditions

and boundaries to overcome the slow SOA gain behavior by improving the gain uniformity are presented. The final section concludes the findings of the investigation.

II. SOA PRINCIPLE OF OPERATION

SOA is an optoelectronic device that can amplify an input light signal under suitable operating conditions. An input signal enters the SOA from the input facet side through the active region where it achieves gain. Gain occurs when an external electric current is applied to supply the energy source to the active region [11]. The SOA is coated with an input and output facets. The amplifier facets are reflective causing ripples in the gain spectrum [12]. Electrons acquire higher energy when the SOA is biased with a direct current. Therefore, applying more bias current will result in a larger number of excited electrons in the conduction band. Applying a short duration input optical pulse into the SOA will result in stimulated emission leading to the signal amplification. The reduction of excited electrons (i.e. carrier density) in the conduction band will lead to a decreased SOA gain. This is because the gain is proportional to the carrier population density. Moreover, this will increase the active refractive index due to the nonlinear refractive index being dependent on the carrier density [13]. The carrier non-equilibrium is governed mainly by the spectral hole burning effect [14]. The distribution recovers to its equilibrium state by the carrier-carrier scattering. Instantaneous mechanisms such as two-photon absorption and the optical Kerr effects [15] will then influence the SOA response. After few picoseconds, a quasi-equilibrium distribution will occur, due to the carrier temperature relaxation process, followed by the carrier density recovery. The SOA gain recovery time is limited by the carriers' lifetime.

III. THEORETICAL MODEL

We have developed a numerical model to analyze the bias current and its effect on the SOA gain. The model is based on position-dependent rate equations for the carrier density and the optical propagation equation in the forward-propagating direction for injected input signals. Therefore, the model accounts for a non-uniform carrier distribution. The complete rate equations in small segments in an SOA are iteratively calculated with 3rd order gain coefficients [16].

Rate Equations

When light is injected into the SOA, changes occur in the carrier and photon densities within the active region that can be described using the rate equations. The gain medium of the amplifier is described by a 3rd order material gain coefficient g (per unit length), which is dependent on the carrier density N and the input signal wavelength λ and is given by [17]:

$$g = \frac{a_1(N - N_O) - a_2(\lambda - \lambda_N)^2 + a_3(\lambda - \lambda_N)^3}{1 + \varepsilon \cdot P_{av}}, \quad (1)$$

where a_1 is the differential gain parameter, a_2 and a_3 are empirically determined constants that characterize the width and asymmetry of the gain profile, respectively. N_o is the carrier density at transparency point, λ_N is the wavelength at which the gain has a peak value, ε is the gain compression factor and P_{av} is the average output power. The peak gain wavelength is given by:

$$\lambda_N = \lambda_O - a_4(N - N_O), \quad (2)$$

where λ_o is the peak gain wavelength at transparency and a_4 is the empirical constant that shows the shift of the gain peak. The net gain coefficient is defined by:

$$g_T = \Gamma \cdot g - \alpha_s, \quad (3)$$

where Γ is the confinement factor which is the ratio of the light intensity within the active region to the sum of light intensity [11] and α_s is the internal waveguide scattering loss.
Therefore, the average output power over the length of the SOA L can be expressed by [18]:

$$P_{av} = P_{in} \frac{e^{g_T \cdot L} - 1}{g_T \cdot L}. \quad (4)$$

where P_{in} is the input signal power. The rate of change of the carrier density within the active region of the device is given by:

$$\frac{dN}{dt} = \frac{I}{q \cdot V} - (A \cdot N + B \cdot N^2 + C \cdot N^3) - \frac{\Gamma \cdot g \cdot P_{av} \cdot L}{V \cdot h \cdot f}, \quad (5)$$

where I is the SOA bias current, q is the electron charge, h is the Plank's constant and f is the light frequency. A is the surface and defect recombination coefficient while B and C are the radiative and Auger recombination coefficients respectively. The active volume is determined by $V = L \times W \times H$ where W and H are the width and thickness of the active region, respectively.

Propagation Equation

The SOA is assumed to have a negligible reflectivity at the end facets, so the reflected waves are omitted. The propagation equation for the forward light is given by [17]:

$$\frac{dP_{in}}{dz} = (\Gamma \cdot g - \alpha_s)P_{in}. \quad (6)$$

IV. RESULTS AND DISCUSSION

The above rate equations (1)-(6) based on the proposed segmentation model is adopted to investigate the gain of the

SOA using Matlab^TM. In this model, the system incorporates a homogeneously broadened traveling-wave SOA, and the input signal mode with narrow linewidths. In the segmentation method, the SOA is divided into fifty equal segments of length l = $L/50$ each, where l is the segment length, and the carrier density is assumed to be constant within each segment. However, the carrier density and the signal power changes from segment-to-segment depending on the input power and the carrier density of the previous segment. The reason that fifty segments were chosen is for a sufficient accurate investigation of the input power effect on the change in the carrier density and the signal gain along the SOA for the intended data rate up to 40 Gb/s.

To calculate the segment total gain and its carrier density, the SOA length L is replaced with l in all the equations given in section III. The pulse power is the peak power of a Gaussian pulse and all signal power is coupled directly to the SOA. The SOA parameters adopted are obtained from [11, 17, 18] and are given in Table I.

Uniform Biasing

For the SOA with uniform biasing, the bias current I is 150 mA. Figure 1 displays the normalized gain response of the SOA when a 1 mW peak power Gaussian pulse with a full-wave-half-maximum (FWHM) of 1.167 ps is launched into the active region. The biasing induced SOA gain rapidly reaches its maximum steady state value within ~1 ns. Energy gained by a large number of electrons from the valence band will help them to overcome the energy gap, thus increasing the number of electrons excited in the conduction band (i.e. carrier density) and therefore increasing the total gain of the SOA. When the input pulse is applied to the SOA at a time ~ 3 ns, it results in a total gain depletion within t_f = 5.83 ps (i.e. the time taken for the pulse to propagate through the waveguide). This is due to the interaction of the input pulse with the excited electrons in the conduction band that leads to the sudden depletion in the carrier density and hence the SOA gain as explained in section II. Following exit of the input pulse from the SOA, the gain shows a slow recovery (t_r ~ 670 ps) back to its steady state value [7].

TABLE I
Physical parameters of the SOA

Parameter	Value
Carrier density at transparency (N_0)	1.4×10^{24} /m^3
Wavelength at transparency (λ_o)	1605 nm
Initial carrier density (N_i)	3×10^{24} /m^3
Signal wavelength (λ)	1550 nm
Internal waveguide scattering loss (α_s)	40×10^2 /m
Differential gain (a_1)	2.78×10^{-20} m^2
Gain constant (a_2)	7.4×10^{18} /m^3
Gain constant (a_3)	3.155×10^{25} /m^4
Gain peak shift coefficient (a_4)	3×10^{-32} m^4
SOA length (L)	500 μm
SOA width (W)	3 μm
SOA height (H)	80 nm
Confinement factor (Γ)	0.3
Surface and defect recombination coefficient (A)	3.6×10^8 1/s
Radiative recombination coefficient (B)	5.6×10^{-16} m^3 /s
Auger recombination coefficient (C)	3×10^{-41} m^6 /s
Gain compression factor (ε)	0.2 /W

Figure 2 shows the normalized SOA gain profile when injected with a burst of 10 Gaussian input pulses separated by 100 ps (10 Gb/s) at 1550 nm. The impact of the pulse burst on the SOA gain is circled in the figure. Prior to injection of the first pulse, the rate equation (5) is almost constant and therefore, the change of the carrier density is neglected. With no input signal, only the 1st and 2nd terms of the (5) are considered as the input power is equal to zero. With the injection of first pulse, the SOA experiences a rapid decrease in the carrier density. This is explained by the 3rd term in (5), which depends on the input power of the pulse and the material gain coefficient, thus causing dN/dt to have a high negative value.

When the pulse exits the SOA, the 3rd term will have a zero value. Therefore, dN/dt will have a positive value and the carrier density will start to increase (i.e. SOA gain recovery). Due to the slow gain recovery of the SOA, the next pulse entering SOA before its full recovery will introduce further gain depletion. This process is repeated until the last pulse exits the SOA.
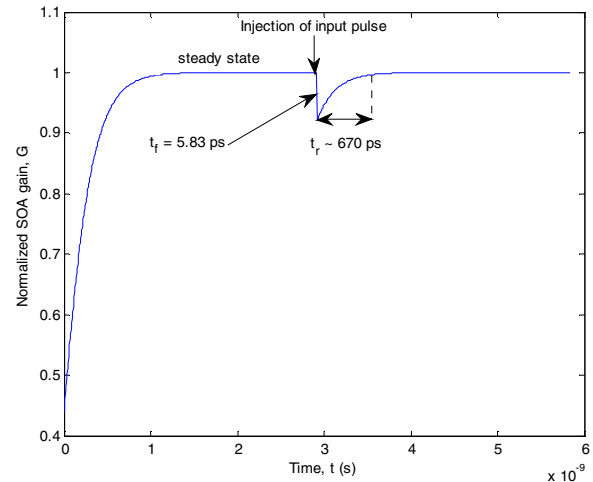

Fig. 1. Normalized SOA gain response to a single input pulse.
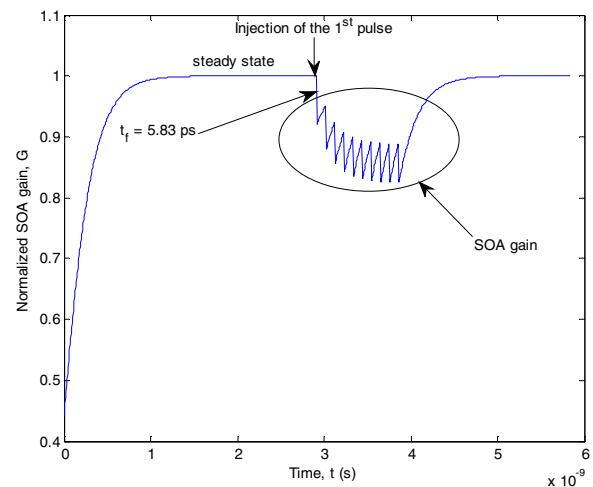

Fig. 2. Normalized SOA gain response to a burst of input pulses.

The gain achieved by the input pulses is proportional to the depletion of the SOA gain. Due to uniform biasing of the SOA, the 1st term of (5) is always constant and therefore, it is not possible to control the changes of the carrier density. The gain standard deviation, which measures the output gain uniformity, can be calculated using the following formula:

$$\sigma = \sqrt{\frac{1}{np}\sum_{x=1}^{np}(G_x - G_{av})^2} \qquad (7)$$

where σ is the gain standard deviation, np is the number of successive input pulses launched into the SOA, G_x is the gain achieved by each input pulse and G_{av} is the average gain of all input pulses. Therefore, in order to minimize σ, i.e. to achieve a flat gain profile, it is important to control the rate of change of N, thus the need for the non-uniform biasing current as proposed in this paper.

Non-uniform Biasing

The non-uniform bias current applied to the SOA has an average value of 150 mA (equivalent to uniform bias current) in order to maintain the same power used in both cases. There are two criteria that control the shape of the bias current applied to the SOA. 1) The need to increase the value of the 1st term of (5) to accelerate the gain recovery. Therefore, a steep increase in the bias current is required following input pulse exist the SOA, to speed-up the SOA gain recovery due to the depletion of N. 2) To maintain the average bias current (power) similar to the uniform bias current (i.e. at 150 mA). Therefore, the bias current should decelerate at the same acceleration rate but in the opposite direction. Hence, a triangular-shape bias current is proposed to meet the required criteria in this paper. For an input signal at a data rate of 10 Gb/s, the bias current is adjusted to the same repetition rate of $1/T$. Over a triangular cycle T of ~100 ps, the bias current can be represented as:

$$I = \begin{cases} m_1 t + C_1 & \text{for} \quad 0 \le t \le T/2 \\ m_2 t + C_2 & \text{for} \quad T/2 \le t \le T \end{cases} \qquad (9)$$
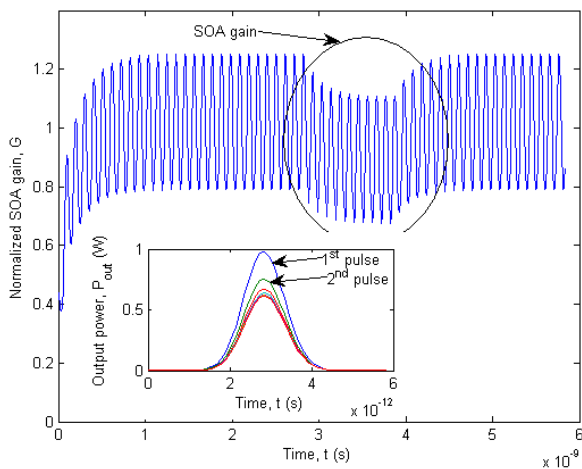

Fig. 3. Normalized SOA gain response to a burst of input pulses using the non-uniform biasing technique and the corresponding profiles of the output Gaussian pulses.

where m_1 and m_2 are the slopes of the triangular signal with values 30.26 and -30.26 mA/ns, respectively. C_1 and C_2 are 70.55 mA and 388.25 mA, respectively. It will take almost 50 ps for the bias current to increase from ~70 mA to 230 mA. For non-uniform biasing, an input pulse stream having the same characteristics as in the uniform biasing case, see Fig. 2, is applied to the SOA. The normalized SOA gain response is illustrated in Fig. 3. From the figure, one can see the oscillations of the SOA gain due to the alternating biasing prior to the injection of the first input pulse. Similar to the uniform biasing technique, the injection of the input pulse causes the SOA gain to drop rapidly within the 5.83 ps. However, in the case of non-uniform biasing, the SOA gain depletion is less effective compared to the uniform biasing. The corresponding profiles of the amplified Gaussian pulses are depicted on the bottom left of Fig. 3. It can be seen that the 1st pulse achieves the maximum gain as expected.

When input signal is launched to the SOA, the 3rd term in (5) is the dominant term. That term is controlled by the time the input pulse is injected to the SOA. There are two different conditions. These conditions can be explained by plotting the change in N within the active region of the SOA for a triangular bias current in Figs. 4 and 5.
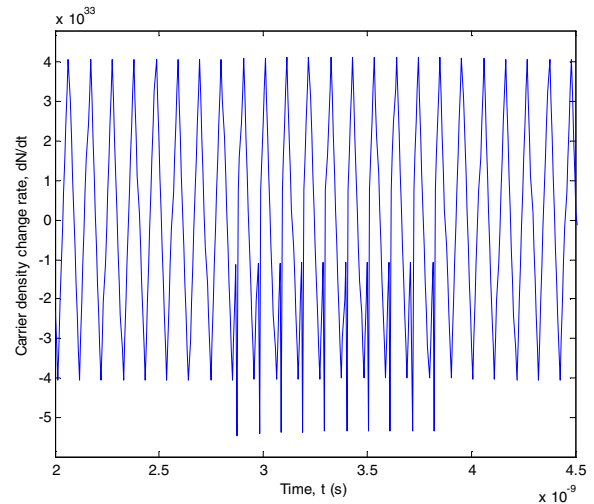

Fig. 4. The change in the carrier density within the active region of the SOA due to non-uniform biasing technique when injected with a burst of input signal at lower carrier density values.
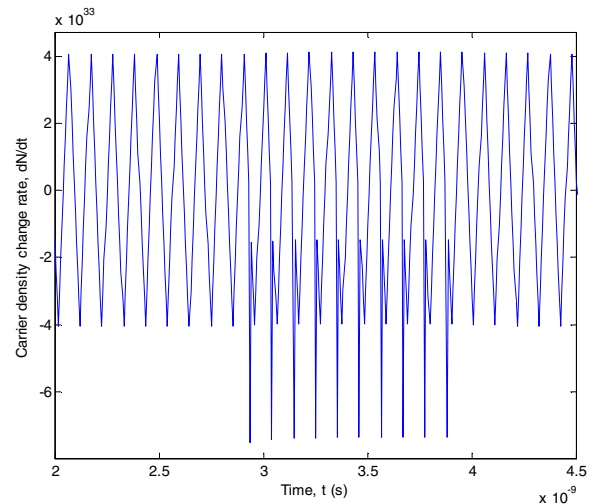
Fig. 5. The change in the carrier density within the active region of the SOA due to non-uniform biasing technique when injected with a burst of input signal at higher carrier density values.

From (1) and (3), one can see the dependence of the material gain coefficient and the net gain coefficient on N. In the first case (see Fig. 4), the 3rd term in (5) will have less impact on the depletion of N and the total gain when the input pulse first enters the SOA at a lower value of N (i.e. the bias current is increasing). Therefore, the effect of the subsequent pulses is minimized resulting in enhanced output gain uniformity.

Figure 6 shows the carrier density of the SOA which is directly proportional to the SOA gain as shown in Fig. 3. On the bottom left of the Fig. 6, one can see that the input pulse is injected at a lower value of N which results in low gain depletion. On the other hand (see Fig. 5), when the input pulse enters the SOA at a higher value of N which can be seen on the bottom right of Fig. 6, higher gain depletion is introduced.

Figure 7 compares σ of the output gain against the power of the input pulse train for uniform and both cases of the non-uniform (for input pulse injection at lower and higher values of N) biasing conditions at 10 Gb/s. At higher input power, the fluctuation of σ is less perturbed. As expected, σ increases with the power of the input signal due to the larger value of the 3rd term in (5). The figure shows that improved gain uniformity compared to uniform biasing is achieved when the input pulses are injected at a lower N values, however, at higher N values less gain uniformity is achieved for all input power levels.

In Fig. 8, we compare the gain standard deviation of the uniform and non-uniform (at lower N value) biasing techniques at higher input data rates (i.e. 20 and 40 Gb/s). The achievement of lower σ at lower data rates is because of the injection of a high speed input pulse train that restricts the full recovery of the SOA gain.
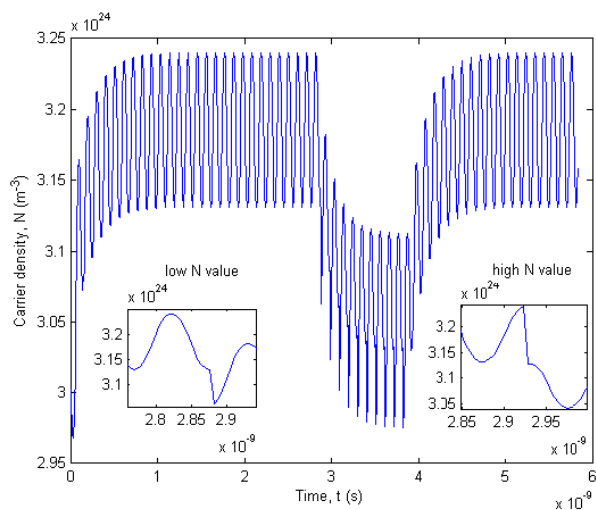

Fig. 6 Carrier density of the SOA when input is injected at lower (bottom left) and higher values (bottom right).
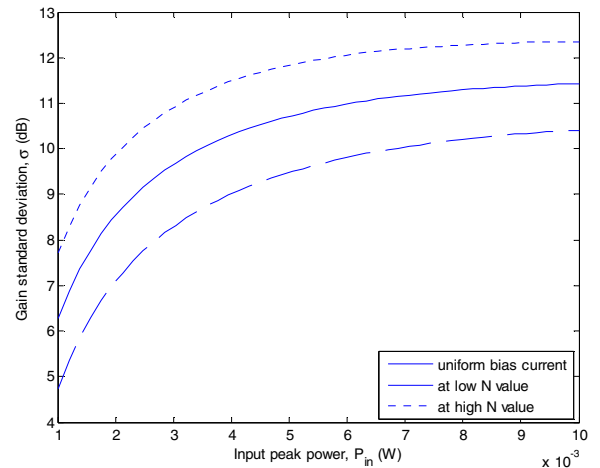

Fig. 7. Comparison of gain standard deviation of uniform and both non-uniform cases (at lower and higher carrier density values) against input peak power of input pulses at 10 Gb/s.
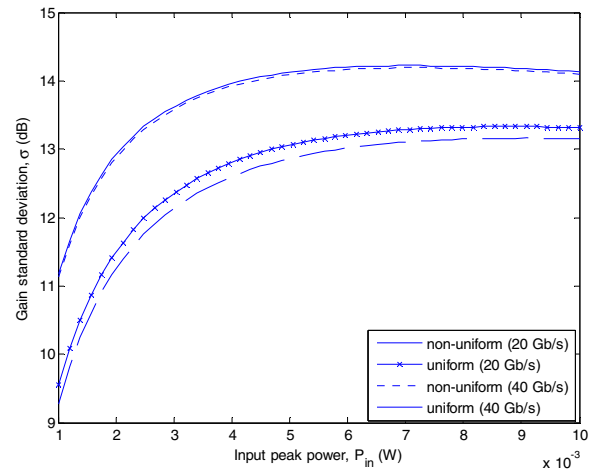

Fig. 8. Comparison of gain standard deviation of uniform and non-uniform cases against input peak power of input pulses at 20 Gb/s and 40 Gb/s.

For example, at 1 mW of input power and for 10, 20 and 40 Gb/s data rates, σ for non-uniform biasing are 4.7, 9.3 and 11.1 dB, respectively, while in case of uniform biasing these are 6.3, 9.6 and 11.2 dB, respectively. For all cases, σ is lower for the non-uniform biasing particularly at 10 and 20 Gb/s data rates. At 40 Gb/s, minimum improvement is achieved. The reason is that, at higher data rates, the output gain has a higher σ due to the reduced pulse period (i.e. short time available for the SOA to recover as a result of each input pulse). Figure 9 presents the difference between σ for uniform and non-uniform biasing schemes against the input signal power for a range of data rates (i.e. the advantage of non-uniform over uniform biasing).
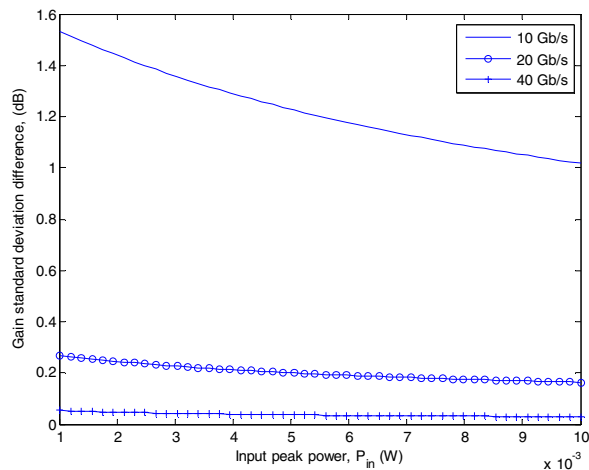
Fig. 9. The difference of gain standard deviation against the input signal power for uniform and non-uniform biasing for a range of data rates

V. CONCLUSION

This paper has proposed a new technique for biasing the SOA. The proposed biasing model is used to enhance the gain uniformity achieved by a train of pulses at different data rates. The total gain response of an SOA model is simulated using a segmentation method. The paper compared the output gain linearity for both uniform and non-uniform biasing techniques. Results obtained show that there is a reduction in the gain fluctuation (i.e. SOA gain reduction and recovery) in case of the triangular shape biasing current compared to the uniform biasing at the condition when the pulses are injected at low carrier density level. It was also shown that an improvement of the gain uniformity is achieved by the input pulses using the proposed non-uniform biasing at 10 and 20 Gb/s data rates. However, the minimum reduction in the gain standard deviation is obtained at 40 Gb/s. Finally there is a need to synchronize the non-uniform biasing with the incoming pulses so that they coincide with low carrier density level which will be addressed in the next stage of this research.

REFERENCES

[1]   T. Durhuus, C. Joergensen, B. Mikkelsen, R. J. S. Pedersen, and K. Stubkjaer, "All optical wavelength conversion by SOA's in a Mach-Zehnder configuration," *IEEE photonics technology letters,* vol. 6, pp. 53-55, 1994.

[2]   R. Giller, R. Manning, and D. Cotter, "Gain and phase recovery of optically excited semiconductor optical amplifiers," *IEEE photonics technology letters,* vol. 18, pp. 1061-1063, 2006.

[3]   E. Tangdiongga, Y. Liu, H. Waardt, G. Khoe, A. Koonen, and H. Dorren, "All-optical demultiplexing of 640 to 40 Gbits/s using filtered chirp of a semiconductor optical amplifier," *Optics Letters,* vol. 32, pp. 835-837, 2007.

[4]   J. Yu, Y. Yeo, O. Akanbi, and G. Chang, "Bi-directional transmission of 8 X 10Gb/s DPSK signals over 80 km of SMF-28 fiber using in-line semiconductor optical amplifier," *Optics Express,* vol. 12, pp. 6215-6218, 2005.

[5]   K. Stubkjaer, "Semiconductor optical amplifier-based all-optical gates for high-speed optical processing," *IEEE Journal on Selected Topics in Quantum Electronics,* vol. 6, pp. 1428-1435, 2000.

[6]   Y. Ben-Ezra, M. Haridim, and B. I. Lembrikov, "Theoretical analysis of gain-recovery time and chirp in QD-SOA," *IEEE photonics technology letters,* vol. 17, pp. 1803-1805, 2005.

[7]   J. L. Pleumeekers, M. Kauer, K. Dreyer, C. Burrus, A. G. Dentai, S. Shunk, J. leuthold, and C. H. Joyner, "Acceleration of gain recovery in semiconductor optical amplifiers by optical injection near transparency wavelength," *IEEE photonics technology letters,* vol. 14, pp. 12-14, 2002.

[8]   H. Ju, S. Zhang, D. Lenstra, H. Waardt, E. Tangdiongga, G. Khoe, and H. Dorren, "SOA-based all-optical switch with subpicosecond full recovery," *Optics Express,* vol. 13, pp. 942-947, 2005.

[9]   C. M. Gallep and E. Conforti, "Reduction of Semiconductor Optical Amplifier Switching Times by Preimpulse Step-Injected Current Technique," *IEEE Photonic Technology Letter,* vol. 14, pp. 902-904, 2002.

[10]   M. H. Lee, S. M. Shin, and S. K. Han, "Wavelength-converting optical space switch using a semiconductor-optical-amplifier-based Mach-Zehnder interferometer," *Optical Engineering.,* vol. 39, pp. 3255-3259, 2000.

[11]   M. Connelly, *Semiconductor optical amplifiers*. New York: Springer-Verlag, 2002.

[12]   G. Keiser, *Optical fiber communication*. Singapore: McGraw-Hill, 2000.

[13]   M. Eiselt, W. Pieper, and H. Weber, "SLALOM: Semiconductor laser amplifier in a loop mirror," *IEEE journal of lightwave technology,* vol. 13, pp. 2099-2112, 1995.

[14]   L. Guo and M. Connelly, "All-optical AND gate with improved extinction ratio using signal induced nonlinearities in a bulk semiconductor optical amplifier," *optics Express,* vol. 14, pp. 2938-2943, 2006.

[15]   G. Agrawal, *Nonlinear fiber optics*, 2 ed. San Diego, USA: Academic Press, 1995.

[16]   J. Mendoza-Alvarez, L. Coldren, A. Alping, R. Yan, T. Hausken, K. Lee, and K. Pedrotti, "Analysis of depletion edge translation lightwave modulators," *IEEE journal of lightwave technology,* vol. 6, pp. 793-807, 1988.

[17]   H. Wang, J. Wu, and J. Lin, "Studies on the material transparent light in semiconductor optical amplifiers," *Journal of Optics A:Pure and Applied Optics,* vol. 7, pp. 479-492, 2005.

[18]   VPIsystems, *VPI transmission maker and VPI component maker: photonic modules reference manual*, 2001.